Chinese Science Bulletin

Scale dependence of direct shear tests

ZHOU Qiang[1,2], SHEN Hayley H[2†], HELENBROOK Brian T[3] & ZHANG HongWu[1]

[1] Department of Engineering Mechanics, Dalian University of Technology, Dalian 116024, China;
[2] Department of Civil and Environmental Engineering, Clarkson University, Potsdam, NY 13699-5710, USA;
[3] Department of Mechanical and Aeronautical Engineering, Clarkson University, Potsdam, NY 13699-5725, USA

Direct shear test has been widely used to measure the shear strength of soils and other particulate materials in industry because of its simplicity. However, the results can be dependent on the specimen size. The ASTM (American Society for Testing and Materials) publications suggest that for testing soils the shear box should be at least ten times the diameter of the largest particle and the height of the box should be no more than half of its diameter. These guidelines are empirically based. A series of two-dimensional numerical direct shear tests are performed to investigate this scaling effect. By analyzing the bulk friction, particle translation and rotation, percentage of sliding, average volume (area) and shear strain and the evolution of the shear band, we find that the traditional guidelines for direct shear tests are questionable. Scaling dependency of bulk friction on the property of granular materials is clearly present. Our current analysis points out that the scaling effects can vary significantly depending on the particle properties other than their sizes. Of all the parameters we observed, particle rotation appears to have a decisive correlation with the bulk friction. Formation of a shear band is universal. As the shearing progresses, particle rotation begins to concentrate near the shear plane. By defining the width of a shear band as the standard deviation of the distribution of translational gradient or the standard deviation of the distribution of particle rotation, quantitative evolutions of shear band are presented. Both measures of the shear band width dropped rapidly during pre-failure stage. After peak stress both measures begin to approach steady state as the bulk friction stabilizes to the residual stage. These observations suggest that structure formation inside the shear band controls the scaling effect.

granular material, direct shear test, scaling effect

The direct shear test combines compression and shear. These two modes of deformation dominate the mechanical behavior of granular materials. The direct shear test is widely used in industry because of its simplicity. For cohesionless materials, the most important data to be obtained from a direct shear test are peak and residual stresses and the friction coefficient corresponding to these two stress states. The accuracy of these measurements is critical to the proper design of structure foundations[1] as well as equipments that handle these materials[2]. The problem that has troubled bulk handling engineers is that the macro-mechanical behavior of granular materials depends on scale. That is, the stress strain relation is not always an intrinsic property but depends on the ratio of the particle size to the sample scale.

In granular materials, scale dependency was observed in direct shear tests, as early as 1936[3]. That study shows that larger shear boxes resulted in smaller friction angle. The ASTM D 3080-90 Standard Test Method for Direct Shear Tests of Soils under Consolidated Drained Conditions stipulates the apparatus size to be at least ten times the size of the largest particle size, and the horizontal dimension of the apparatus to be at least twice the vertical dimension. However, recent studies question

Received March 20, 2009; accepted June 30, 2009; published online September 10, 2009
doi: 10.1007/s11434-009-0516-5
†Corresponding author (email: hhshen@clarkson.edu)
Supported by the ASEE/NASA Summer Faculty Fellowship Program and Clarkson University

Citation: Zhou Q, Shen H H, Helenbrook B T, et al. Scale dependence of direct shear tests. Chinese Sci Bull, 54: 4337−4348, doi: 10.1007/s11434-009-0516-5

this rule of thumb. For example in the study by Cerato and Lutenegger[4], size dependence was found to be present despite adherence to the ASTM guidelines. It was consequently suggested that the apparatus size be from 20 to 150 of the particle size, depending on the materials tested.

From a practical point of view, a small apparatus to particle size ratio has great advantage because it reduces the specimen needed for testing. From a computational point of view, a small apparatus to particle size ratio means fewer particles to simulate. In most cases, it is impossible to simulate the real particle system due to a large number of particles in any practical industrial process. Thus, coarsening of particles is required. To properly coarsen granular materials we need guidelines on how to enlarge particle size while maintaining the fidelity of the mechanical behavior. Otherwise computational tools for such systems are still far from reliable for practical applications.

The mechanisms leading to scale dependency in dense granular materials are not well-understood. Many apparent structures exist in dense granular systems such as fabric tensor, void tensor, force chains and stiffness matrix. Mathematical descriptions have been developed for fabric and void tensors[5–9]. For force chains[10] and stiffness matrix[11] such development has also begun. Statistical distribution of structures and their evolution during shear is a topic of some recent publications[12,13].

To address the source of scale dependency in direct shear tests, detailed 2D DEM simulations are performed. Both particle level and continuum quantities are investigated: slipping contact percentage, particle displacement and rotation, and shear and dilatation distribution. Different size particles are used in a fixed size direct shear cell. Different size shear box tests are performed as well. The aim is to determine if any of these internal parameters investigated can shed some light on the mechanisms leading to scale dependency.

1 Bulk friction

Figure 1 is a schematic of a 2D direct shear box. There is a constant normal load on the lid, which is free to move up and down. However, rotation of the lid is prohibited in the numerical experiment. The two horizontal side walls prevent the particles from falling out of the box once shear begins. The particles are generated randomly inside the box with an initial size 83% of their

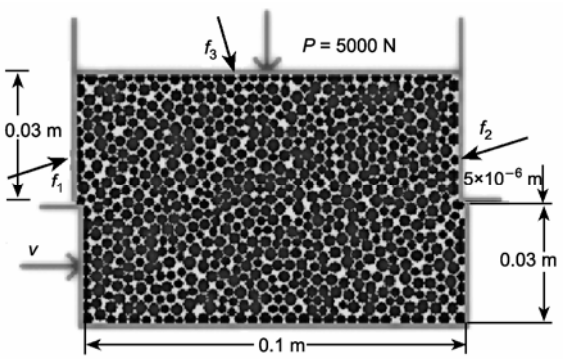

Figure 1 The direct shear test schematic. The maximum shear displacement is 0.01 m.

real diameters. After all particles are generated, each particle is given a random initial velocity. Then three things happen simultaneously: The particles diameters grow, they move under the influence of gravity, and they interact with each other through contact mechanics. After all particles grow to their final size, a settling period is simulated to reach the equilibrium under the applied normal load. The direct shear test is then performed by translating the bottom half of the box while keeping the top half stationary.

The bulk friction, μ, which is one of the key parameters used to describe the macro-mechanical property of granular materials, is given by

$$\mu = f_s / f_n, \tag{1}$$

where f_s and f_n are the shear and normal forces acting on the shear plane. If the inertia effect is neglected, the shear force f_s equals the horizontal contact forces between the particles and the box ($f_s = f_1^t + f_2^t + f_3^t$) and the normal force f_n equals the vertical contact forces between the particles and box plus the material weight above the shear plane ($f_n = f_1^n + f_2^n + f_3^n + W$). In the following, we use the boundary forces and the weight of the materials in the top half of the box to calculate the bulk friction. A discussion of the evolution of boundary and internal stresses may be found in ref. [14].

A linear contact model is used to calculate the contact force between particles and particles with walls[15,16]. The contact forces between a contact pair $\{i, j\}$ are given as

$$\begin{aligned} F_{n_{ij}} &= k_n \delta_{ij} n_{ij} - 2\zeta_n (k_n m_e)^{1/2} v_{n_{ij}}, \\ F_{t_{ij}} &= \min\left(\mu_s F_{n_{ij}}, \int_0^t k_t v_{t_{ij}} \mathrm{d}t \right), \end{aligned} \tag{2}$$

where $k_{n,t}$ is the elastic constant and $\zeta_{n,t}$ is the damping ratio in the normal direction, respectively; δ_{ij} is the normal compression, n_{ij} is the normal contact vector, $m_e = m_i m_j/(m_i+ m_j)$, μ_s is the sliding friction coefficient, $v_{n_{ij}}$ and $v_{t_{ij}}$ are the relative normal and tangential velocities between the two particles, respectively; t is the duration of contact or the time when friction limit is reached, whichever comes first. There is no damping in the tangential direction.

To investigate the scaling effect, a series of numerical direct shear tests have been performed. Different size particle assemblies have been generated in the box, then loaded and sheared. Because uniform size particles tend to form crystallized packing pattern, we used a size distribution. To concentrate on the size effect but not the size distribution effect, we assume a normal distribution with a standard deviation at $0.5d_{\mathrm{m}}$, where d_{m} is the mean particle diameter. All other parameters are kept constant (Table 1). This normal distribution is cutoff between $0.8-1.2d_{\mathrm{m}}$.

Due to the stochastic nature of the system, each case is simulated 10 times with a different initial packing. The average bulk friction values obtained from the 10 samples for each case are shown in Figure 2. It is clear that different size particles in the same size box generated different results. In soil mechanics terminology, the "pre-failure" stage corresponds to the rising part of the bulk friction curve. The "peak stress" and "residual stress" correspond to the stresses at the maximum bulk friction and at the final leveled off stage[17], respectively. Due to the stress fluctuations it is difficult to pinpoint the peak and the residual bulk friction. Thus the peak bulk friction is defined to be the mean of the friction values within an interval of ±1% of the total displacement from the maximum friction obtained from the average of the 10 tests. The residual friction is defined as the mean of the last 20% of the displacement from the average of the 10 tests. In case of soil, if a specimen is densely packed, all three stages should be present under direct shear. For loosely packed specimen the bulk friction approaches failure without experiencing the peak stress stage. Results shown in Figure 2 indicate that all specimens were densely packed. The mean values of the peak and residual friction values together with their standard deviation are shown in Figures 3 and 4. From these results we notice the following:

(i) The rise of the bulk friction to the peak stress is scale-dependent. For the cases studied, larger particles have higher pre-failure stress and peak stress.

(ii) The peak friction depends on the particle size but the standard deviation is less sensitive to particle size (Figure 3). The standard deviation is defined as

Table 1 Parameters used in the simulations[a)]

Box height (m)	Box length (m)	Contact stiffness ($\times10^6$ N/m)	Density ($\times10^3$ kg/m^3)	Restitution coefficient	Friction factor (particle-particle)	Friction factor (particle-side walls)	Friction factor (p-top/bottom walls)	Shear displacement (m)	Total mass (kg)	Top load force (N)
0.06	0.1	5.8	2.545	0.7	0.5	0.2	1.0	0.01	12.6	5000
0.03	0.1	5.8	2.545	0.7	0.5	0.2	1.0	0.01	6.3	5000

a) The contact parameters between particles and walls are the same as between particles.

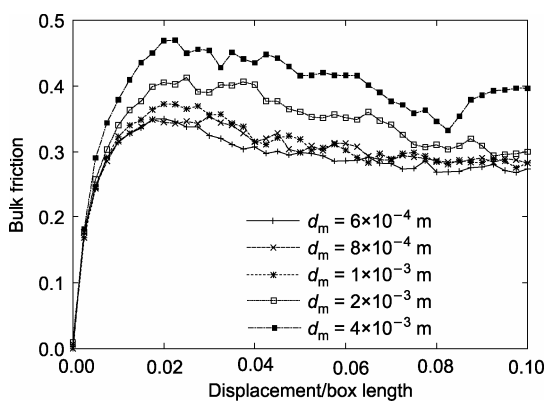

Figure 2 The average bulk friction curves of different particle size assemblies.

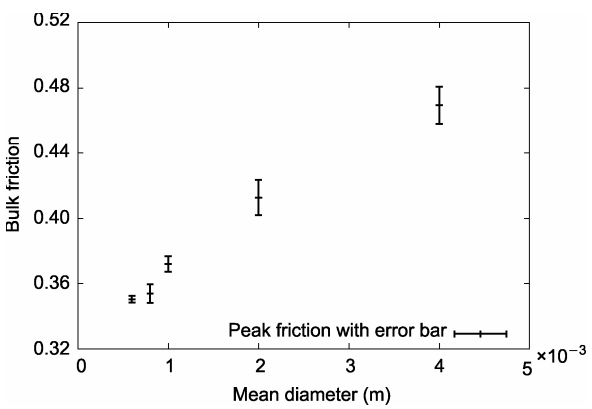

Figure 3 The mean and standard deviation of peak friction of different size assemblies.

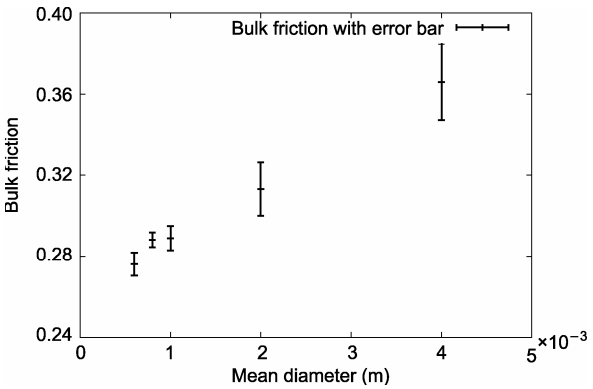

Figure 4 The mean and standard deviation of residual friction of different size assemblies.

$$\sigma = \sqrt{\frac{1}{n-1}\sum_{i=1}^{n}(x_i - \bar{x})^2}, \tag{3}$$

where n is the number of data points within ±1% of the peak friction from Figure 2 and $\bar{x}$ is the average within this range.

(iii) The residual friction has the same trend as the peak friction. Namely larger particle size results in greater residual stress. The mean and standard deviation are calculated using data points within the last 20% of displacement from each case in Figure 2.

2 Internal parameters

We now study the internal parameters during the shear process. To characterize the trend of displacement over 10 cases, of which the particles are generated randomly, the whole domain is split into 0.01 m by 0.01 m non-overlapping subdomains in all cases. The spatial distribution of several internal variables is presented below. Contours of these variables are obtained using data from the fixed matrix of subdomains.

(i) Horizontal displacement. The average horizontal displacement of particles within each subdomain is shown in Figure 5. A clear transition zone can be seen. This result is expected from previous direct shear and biaxial tests[4,18]. Notice that this zone of the small size assemblies in Figure 5(a) is narrower than the one of the larger size particle assemblies in Figure 5(b). Moreover, the mode of motion in the direct shear box is not purely horizontal. The contour plots of the vertical displacements in Figure 6 clearly show strong localized vertical motion. The formation of shear bands has been studied extensively both experimentally and theoretically[19,20]. Except that the shear band width is on the order of ten particle diameters, the results of these studies are not conclusive. In addition, although shear bands are visually evident, it requires a definitive criterion to quantify their sizes. Discontinuity of shear gradient has been used. However in practice due to the noise of the kinematics at the particle level and necessary smoothing, discontinuities are never sharp. As will be presented later, we will use a standard deviation as a measure of the width of a shear band.

(ii) Volume and shear strains. The strain of the granular materials in the shear box is studied next. For a discrete system Cundall and Strack[15] introduced the

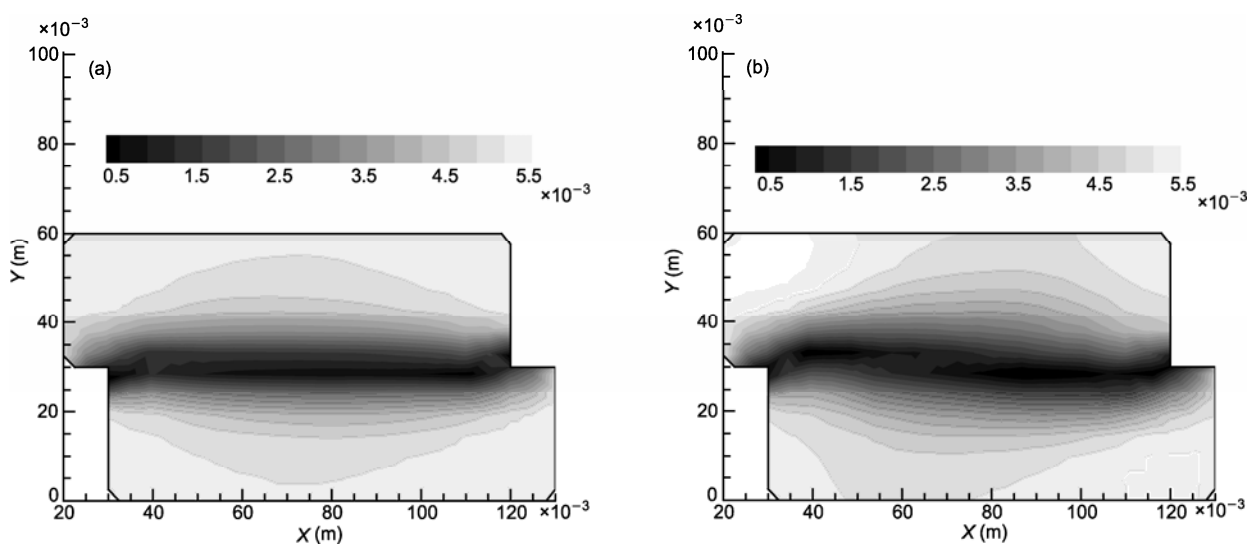

Figure 5 Contours of |X–5| when shear displacement reaches 0.01 m, where X (m) is the local horizontal displacement. (a) d_m = 0.001 m; (b) d_m = 0.004 m.

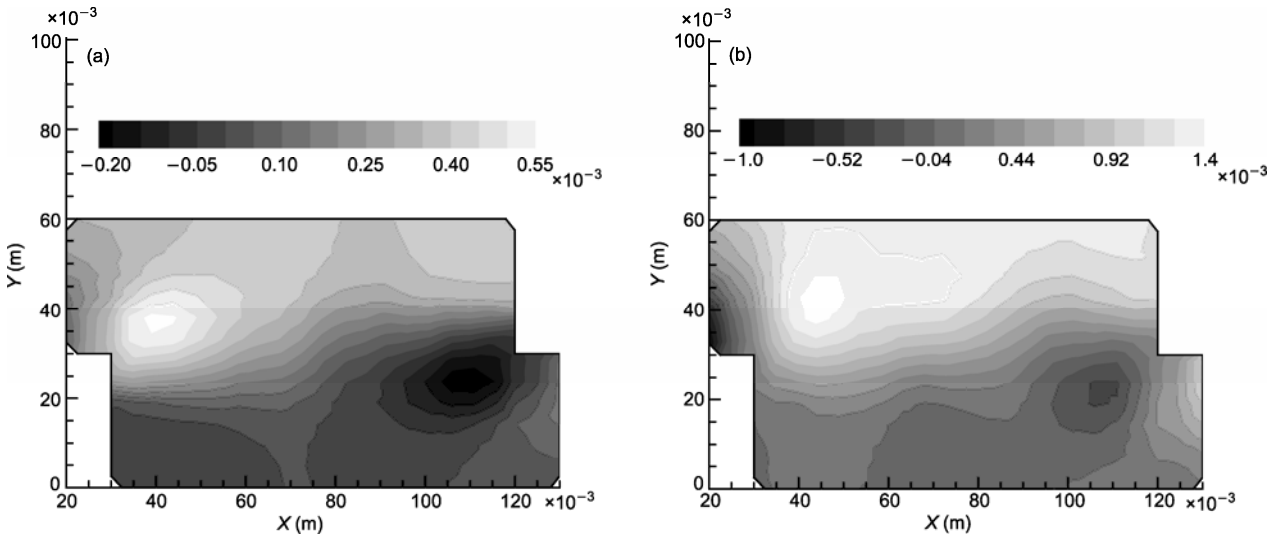

Figure 6 Contours of *Y* displacement of granular materials within the box when the shear displacement reaches 0.01 m. (a) d_m=0.001 m; (b) d_m=0.004 m. Instead of keeping constant for both cases, the range of these contours in this and subsequent figures is optimized to show the details within the shear cell in each case.

following definition for the strain ε_{ij} field:

$$\varepsilon_{ij} = z_{ij} \sum_{p=1}^{n} du_j^p x_k^p, \tag{4}$$

where n is the number of particles in the region of concern, x_k^p is the position of particle p, du_j^p is the relative translation of particle p with respect to the average translation in the subdomain. The coefficients z_{ij} are obtained through linear regression. Using this definition, the resulting dilatation $\varepsilon_{11}+\varepsilon_{22}$ is given in Figure 7 and the maximum shear strain $\varepsilon_{11}-\varepsilon_{22}$ in Figure 8 for the end of shear condition. Both quantities show the band structure in the displacement field. Again the band formation is more distinct in the small particle case. The dilatation of the larger particles is greater than the smaller ones.

(iii) Percentage of sliding contact. For frictional materials, sliding is the mode of "failure" at the grain level in the absence of rolling friction. We will study the sliding contacts in the shear tests next. The percentage of sliding contacts in a subregion is defined as

$$\zeta = N_s / N_a, \tag{5}$$

where N_s is the number of sliding contacts, and N_a is the number of all contacts in the subregion. As the particle displacement in the previous section, N_s and N_a are the

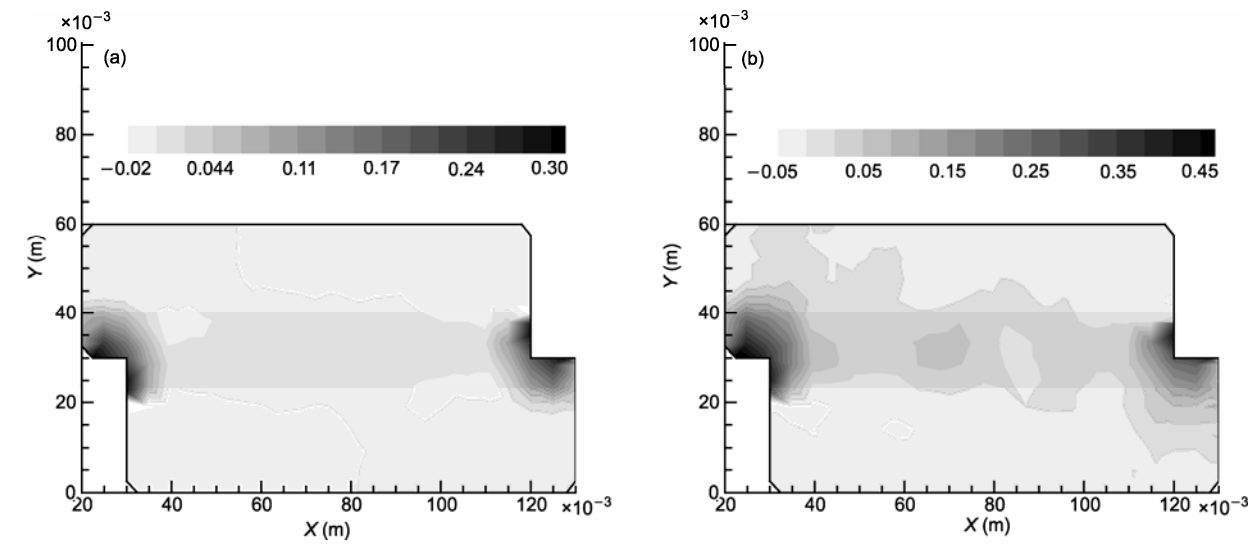

Figure 7 The comparison between the volumetric strain in a 0.06 m height box. (a) d_m=0.001 m; (b) d_m=0.004 m.

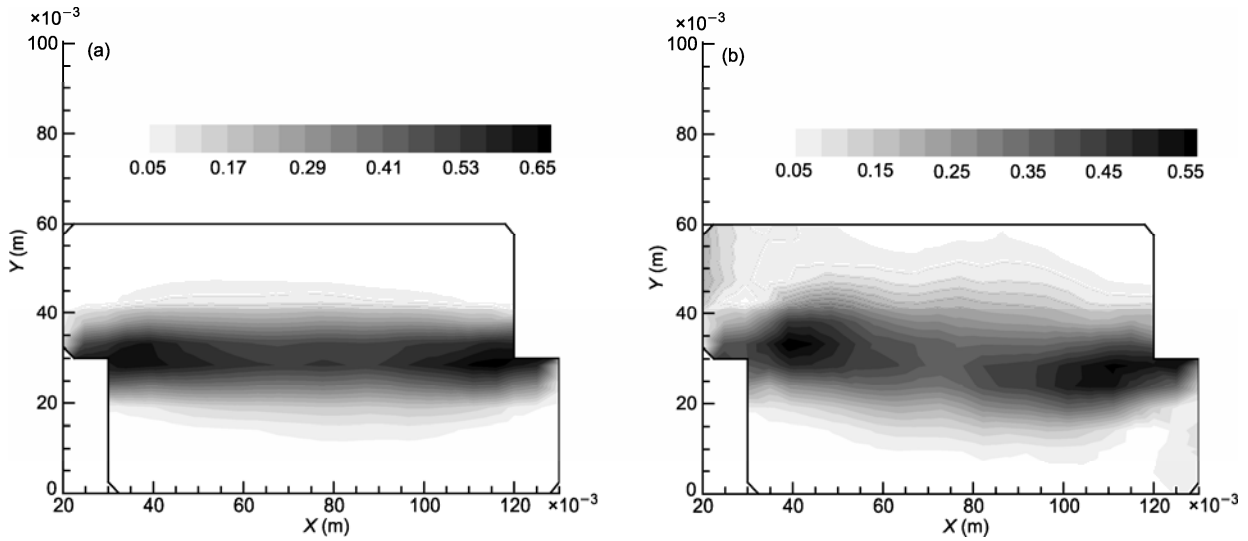

Figure 8 The comparison between the maximum shear strain in a 0.06 m height box. (a) d_m=0.001 m; (b) d_m=0.004 m.

respective averaged values over 10 cases. The results of sliding contacts are shown in Figures 9 and 10. Initially ζ is small and quite uniformly distributed. As the shear develops ζ concentrates on the shear plane. The same happens in a biaxial test[21]. Even at the beginning of the shear far from reaching the peak stress, there was already sliding in the shear box, implying that there was no pure elastic regime.

(iv) Particle rotation. It is surprising that even when the shear is fully developed towards the end ζ is only a few percent in all cases. Apparently the granular material accommodates shearing by another mode of relative motion. The other mode of relative motion is an organized particle rotation. Figure 11 shows the distribution of particle rotation inside the box. A clear band surrounding the shear plane again forms. This band is also dependent on the particle size, as in all previously shown parameters.

(v) Effect of box size and aspect ratio. Cerato and Lutenegger[4] used five types of sand to test the specimen size and scale effects of the direct shear test, focusing on the particle-size to box-size ratios. They observed that small particle-size to box-size ratios provided a smaller friction angle. They showed that not only the relative size of the particle to the box but also the aspect ratio affected the bulk friction. From dimensional analysis one would expect that changing the box size but fixing the aspect ratio is equivalent to changing the relative

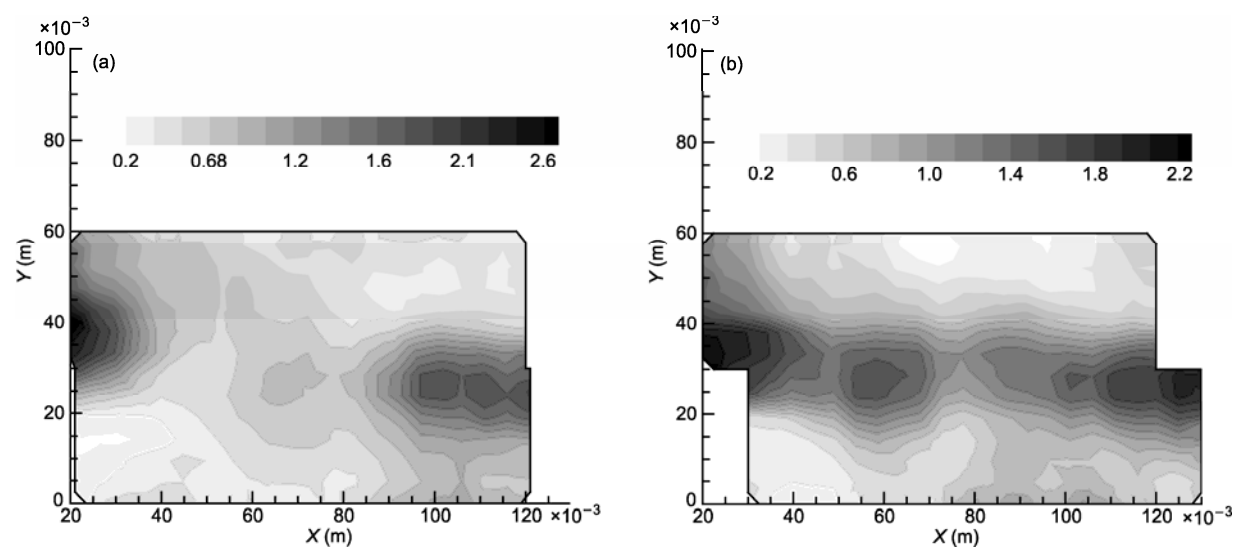

Figure 9 The contours of slip percentage of d_m=0.001 m particle assemblies. (a) At the beginning of the shear; (b) at the end.

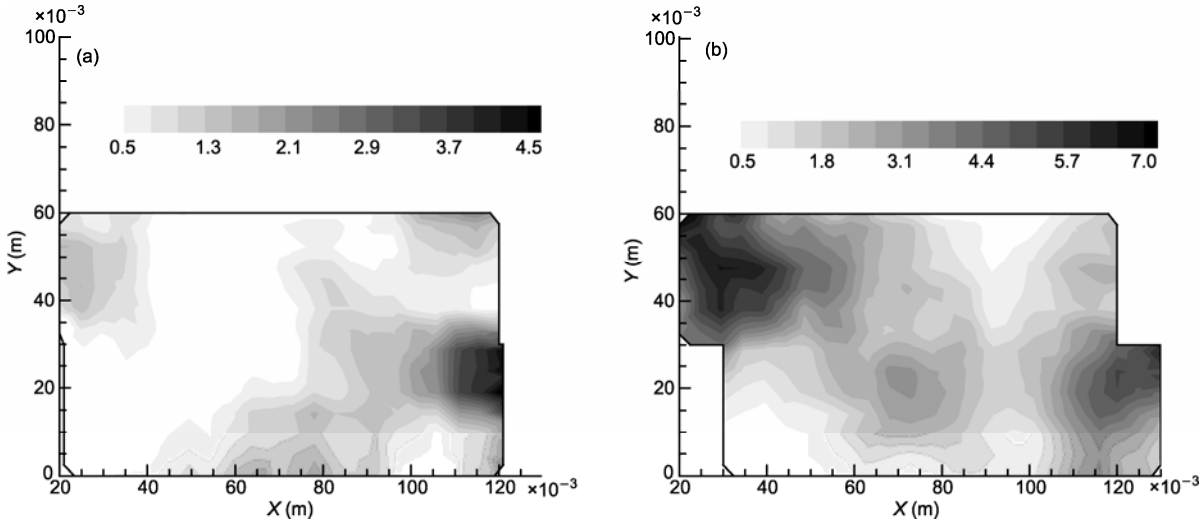

Figure 10 The contours of slip percentage of d_m=0.004 m particle assemblies. (a) At the beginning of the shear; (b) at the end.

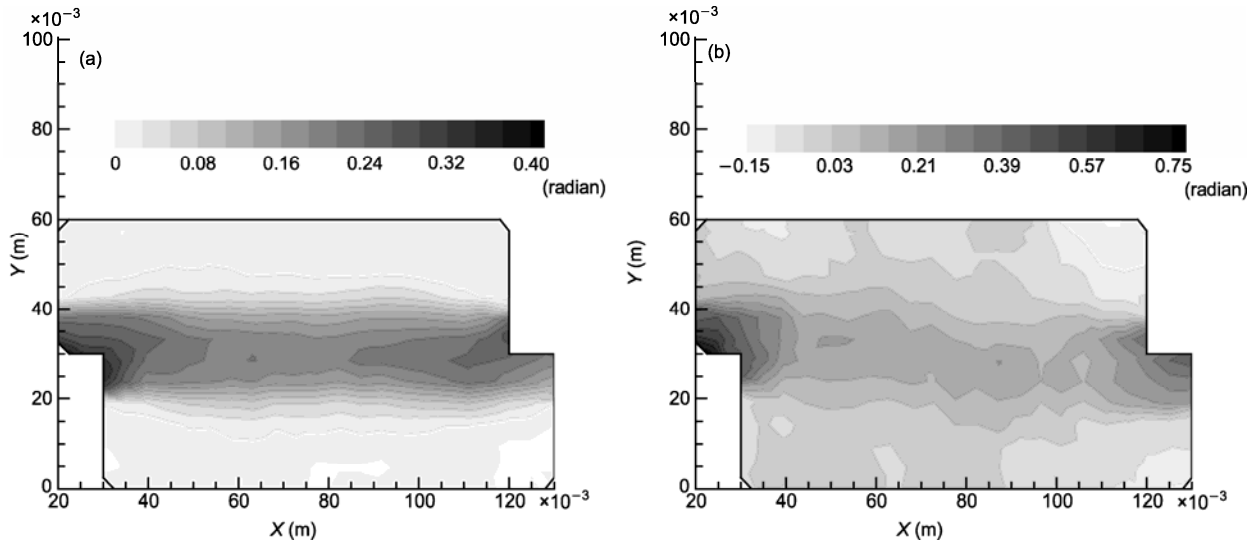

Figure 11 The comparison between average particle rotation in a 0.06 m height box. (a) d_m=0.001 m; (b) d_m=0.004 m

size of the particles to the box size. To verify this idea, a series of numerical tests have been performed. In each case particle size and all other parameters are kept the same but the width and height of the box are varied while fixing the aspect ratio. As shown in Figure 12 the results confirm that changing the box size has the same effect as changing the particle size if the aspect ratio and all other parameters are fixed.

To test the effect of aspect ratio we change the box height from 0.06 m to 0.03 m. We note that in order to adhere to the ASTM recommendation, despite the difference between a 2D and a 3D situation, the box height for a 0.1 m diameter box should not exceed 0.05 m. As shown in Figure 13, the average bulk friction curves of

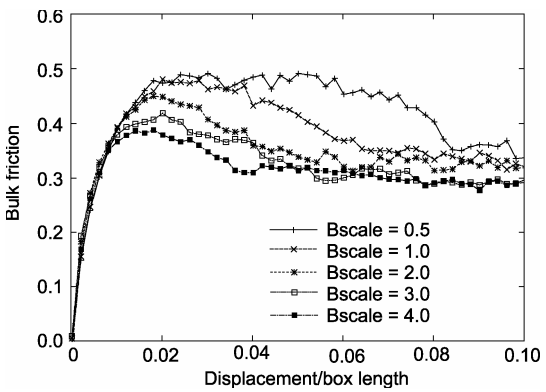

Figure 12 The average bulk friction of same size particle assemblies in different size boxes with the same aspect ratio, where Bscale is the length of the scaled box divided by the baseline length in Figure 1.

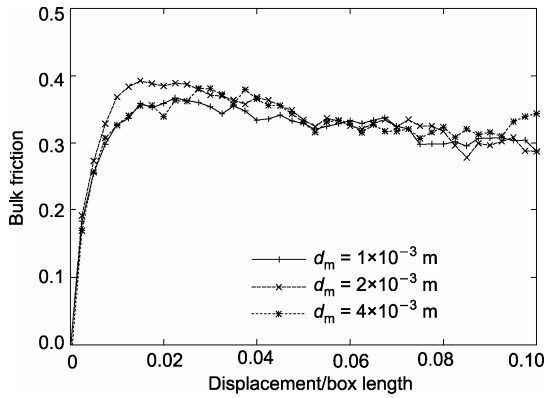

Figure 13 Average bulk friction of different size assemblies in a 0.03 m height box.

particle size from d_m= 0.001 m to d_m= 0.004 m merge. It seems that the scaling effect vanishes and bulk frictions all converge to the case with small particles shown in Figure 2. Figure 14 shows the average horizontal displacement in the direct shear box from 10 tests. By comparing the contours in Figure 14(a) and (b), the difference between displacements of two different sizes is not so much as in the 0.06 m high box. Unlike in the 0.06 m high box, the shear band now extends to the top and bottom walls for both small and large particle cases. Thus shearing of the granular material is now a combined effect from the material itself and the boundaries.

(vi) Effect of rolling friction. Circular particles are very special cases. Typical natural or man-made particles usually have surface roughness resulting in multiple contact points between two particles simultaneously. One immediate consequence of this multiple contact is the resistance to relative rotation, because any rotational tendency will produce non-uniform force distribution and thus a resisting torque. Iwashita and Oda[22] proposed a contact model with rolling resistance in the biaxial simulation of granular materials. This simple model allows for inclusion of rolling resistance even for single-point contact such as between two circular particles. The contact model provides an additional torque

$$M_r = k_r \theta_r, \tag{6}$$

where k_r is the rolling stiffness, and θ_r is the relative rotation between the two particles. Like the maximum value of static friction, this torque is capped by a threshold determined by the rolling friction coefficient μ_r

$$|M_r| \le \mu_r N, \tag{7}$$

where N is the normal force between the contact pair.

Both sliding and rolling friction (μ_s, μ_r) affect the bulk friction of granular materials. Estrada and Taboada[13] analyzed the bulk friction of a 2D simple shear flow of dense granular materials. They produced a map of the bulk friction in terms of different combinations of μ_s and μ_r (where μ_r was made dimensionless by dividing by the sum of contacting radii). Their map consisted of L-shape contours indicating regions of sensitivity to exclusively μ_r or μ_s, and regions of sensitivity to both coefficients. We now study the effect of rolling friction in a direct shear configuration. Figure 15 shows the average bulk friction curves for two different rolling friction coefficients: μ_r= 10^{-4} m and μ_r= 10^{-7} m. Comparing with the

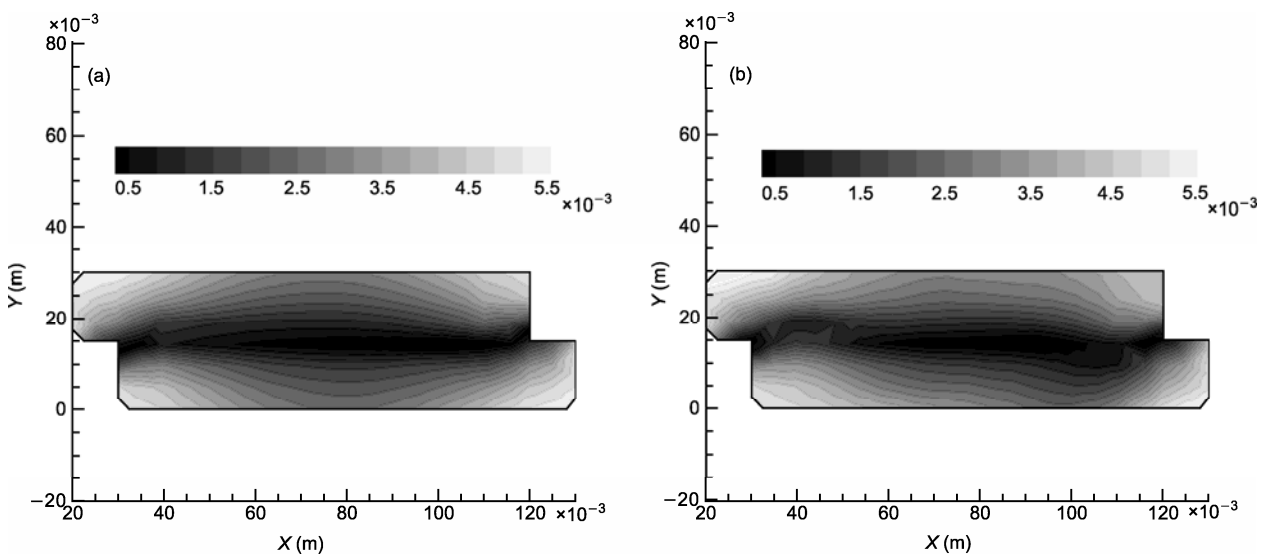

Figure 14 Contours of |X–5| in a 0.03 m height box when shear displacement reaches 0.01 m, where X (m) is the local horizontal displacement. (a) d_m=0.001 m; (b) d_m=0.004 m.

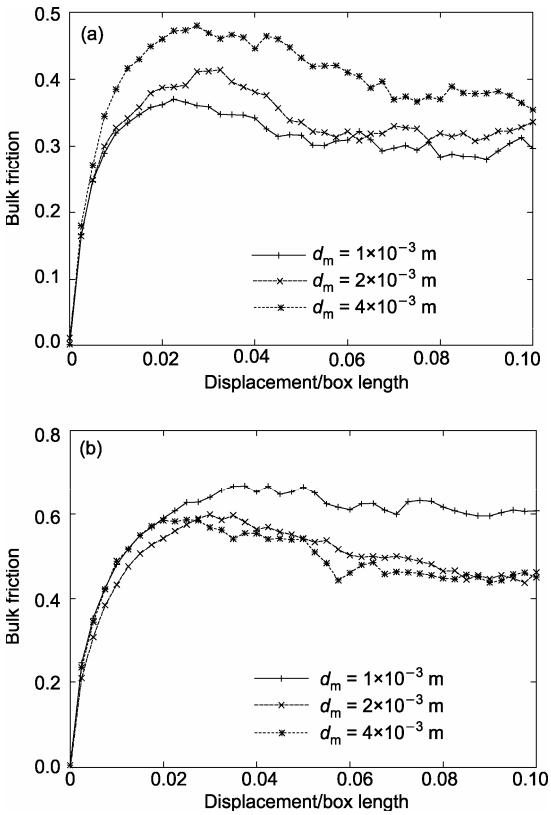

Figure 15 Average bulk friction for μ_r=1×10^{-7} m (a) and μ_r=1×10^{-4} m (b).

curves without rolling resistance as shown in Figure 2, we observe that both peak and residual friction increase. For μ_r= 10^{-7} m this increase is negligible. For μ_r= 10^{-4} m the trend of particle size dependence of the residual bulk friction is now opposite to that in Figure 2, i.e. small particles now exhibit higher residual bulk friction. On the other hand, the peak bulk friction for this case appears to have no size dependence. We believe that higher μ_r will lead to an opposite trend shown in Figure 2 for both peak and residual bulk friction.

3 The width of a shear band

As mentioned earlier, shear band formation has been observed previously in numerous studies. Although clearly visible, a quantitative definition of what constitutes the interior of a shear band is lacking. Iwashita and Oda[22] showed that inside a shear band particle rotation was much greater than the outside region and the packing density was also much lower. Bardet and Proubet[23] showed that translational motion was much more pronounced inside the shear band. All of these parameters may be used to quantitatively define the width of the shear band. In order to have a consistent definition to measure the width of a shear band, we adopt the following standard deviation formula where a shear band width related to particle rotation is defined as

$$w_r = \sqrt{\sum_{p=1}^{N_p} \frac{1}{N_p - 1}(y_p - y_m)^2 \frac{\theta_p}{\bar{\theta}}}, \tag{8}$$

in which N_p is the number of particles in the shear box, y_p is the particle vertical coordinate, y_m is the shear plane position, θ_p is the rotation of a particle, and $\bar{\theta}$ is the average particle rotation of the whole domain. Based on the same idea, a shear band width relating to the gradient of the horizontal (x) displacement is defined as

$$w_g = \sqrt{\sum_{s=1}^{N_s} \frac{1}{N_s - 1}(y_s - y_m)^2 f}, \tag{9}$$

where N_s is the number of subdomains, y_s is the subdomain's vertical coordinate, f is the horizontal displacement gradient at location y_s. Both eqs. (8) and (9) can be used to define the shear band. In a similar fashion, shear band width may be defined using any of the internal parameters studied here. We will however investigate only the rotation and translational gradient and determine which one is more clearly correlated with the bulk friction development.

In Figures 16 and 17 we plot w_r and w_g together with the bulk friction for two different rolling friction values μ_r= 10^{-4} m and μ_r= 10^{-7} m, respectively. These results are obtained using the box dimension shown in Figure 1. At the beginning of shear w_r is large, which means that there is no shear band, and the amplitude of particle rotation has a uniform distribution everywhere. As the shear progresses, both w_r and w_g drop, indicating the formation of a well-defined shear band.

Comparing Figures 16 and 17, it can be seen that the width of a shear band defined as w_r is sensitive to the value of rolling friction. When μ_r= 10^{-7} m, w_r is narrower than it is when μ_r= 10^{-4} m. We believe that higher rolling friction prohibits particle rotation and hence more particles need to coordinate their motion in the vertical direction to accommodate the shearing of the box, thus widening the shear band.

Finally we present the solid area fraction (or 1-porosity) in Figure 18. We observe that in all cases the samples were overconsolidated at first. The expansion of the sample as the shear band develops and approaching to steady state is present in all cases. The expansion is greater for μ_r = 10^{-4} m than it is for μ_r= 10^{-7} m.

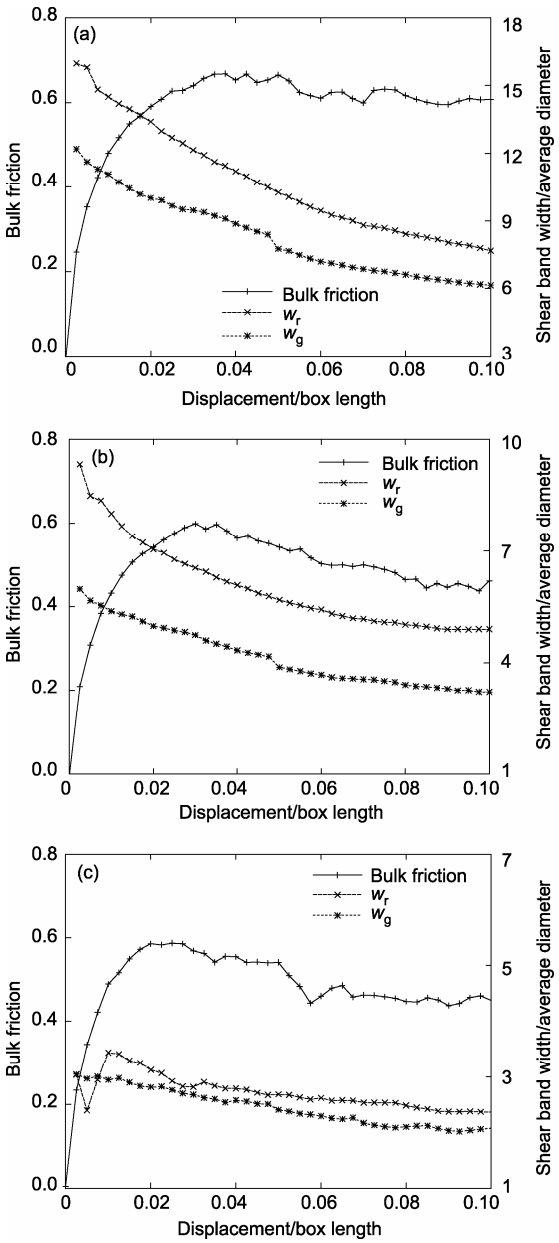

Figure 16 The evolution of bulk friction, w_r and w_s during shear for $\mu_r = 10^{-4}$ m. (a) d_m=0.001 m; (b) d_m=0.002 m; (c) d_m=0.004 m.

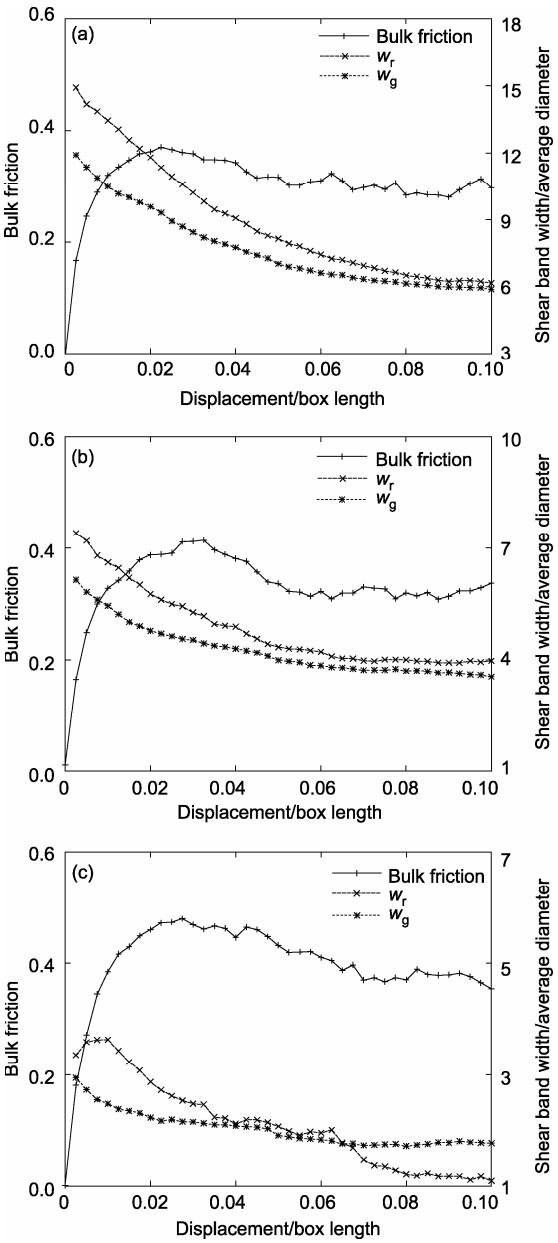

Figure 17 The evolution of bulk friction, w_r and w_s during shear for $\mu_r = 10^{-7}$ m. (a) d_m=0.001 m; (b) d_m=0.002 m; (c) d_m=0.004 m.

4 Discussion and conclusion

We presented a series of 2D numerical tests in a direct shear box. Our primary goal is to investigate the scaling behavior in direct shear tests. The parameters tested are particle size, aspect ratio of the box and the effect of rolling friction. Many of the phenomena found in this study were also observed extensively in biaxial tests of granular materials. These include the formation of shear band, the dependence of the shear band on the particle size, and the dependence of the bulk friction on the particle size. Our results also verified that both length and height of the box affect the bulk friction as found in a recent study using physical tests[4]. However, there are two surprising observations:

(i) The ASTM recommended box size in fact may result in shear band reaching the box boundaries.

(ii) Smaller particle/box ratio may either decrease or increase the bulk friction. The rolling friction plays a strong role here.

Concerning the first observation, we note that direct and biaxial shear tests begin with micro shear bands dis-

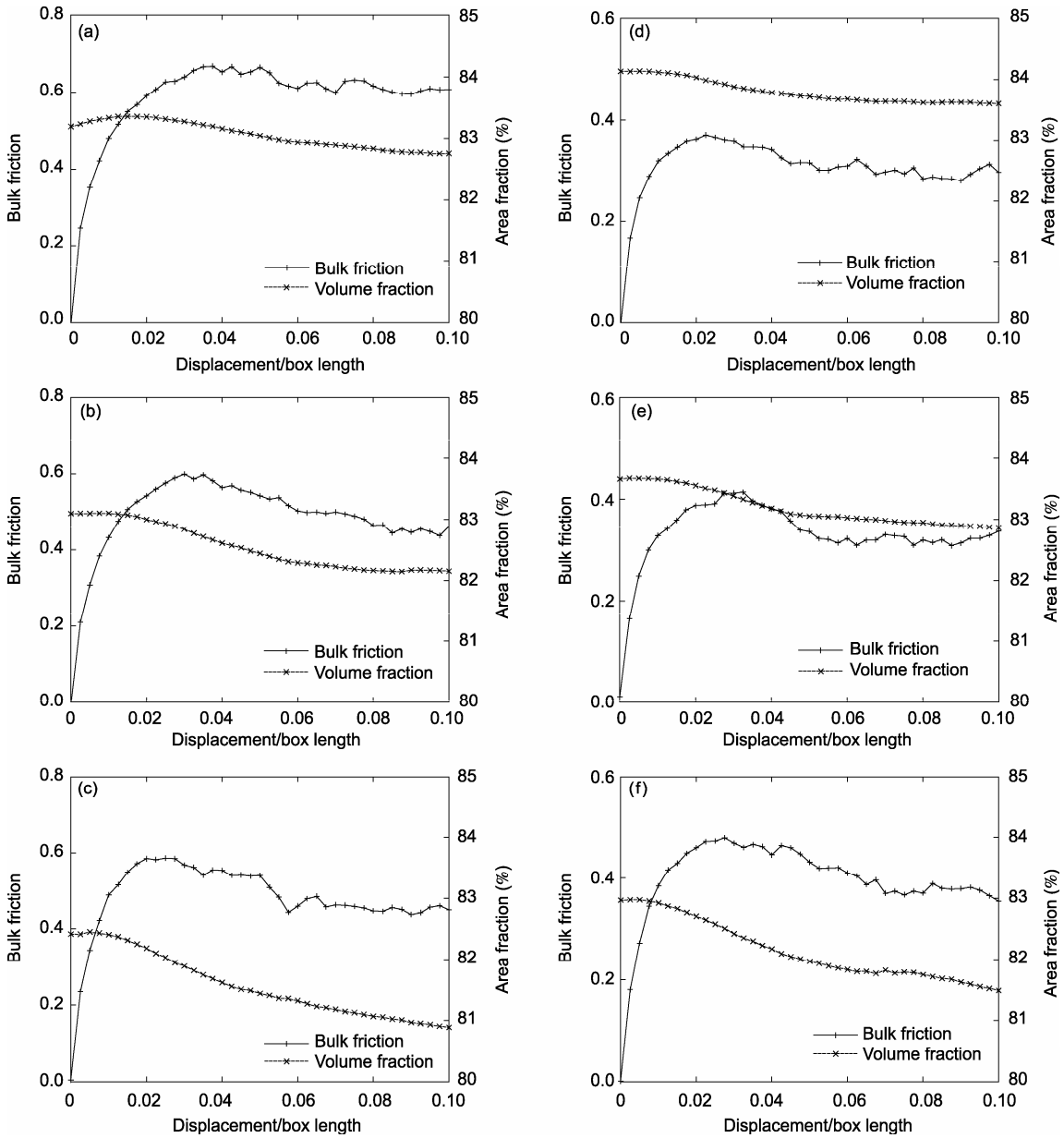

Figure 18 The evolution of bulk friction and the solid area fraction during shear. (a) d_m=0.001 m, μ_r=10^{-4} m; (b) d_m=0.002 m, μ_r=10^{-4} m; (c) d_m=0.004 m, μ_r=10^{-4} m; (d) d_m=0.001 m, μ_r=10^{-7} m; (e) d_m=0.002 m, μ_r=10^{-7} m; (f) d_m=0.004 m, μ_r=10^{-7} m.

tributed in the granular assembly[24]. Given sufficient shear strain, these micro shear bands coalesce into a major shear band[21]. The close correlation among particle rotation, shear band formation and the development of shear stress as shown in Figures 16 and 17 suggests that shear band formation may be the source for scaling laws in granular materials. If true, the influence of boundary is part of the scaling law.

Concerning the second observation we speculate that column-like structures inside the shear band are responsible for the majority of the shearing load. These structures periodically form, rotate and collapse. This idea has been suggested by many other authors in studying biaxial tests[25]. Our current data show that such structures and their stability may be strongly affected by rolling friction as well as the boundaries. It is puzzling why the trend of bulk friction dependence on the ratio of particle/box size would reverse when the rolling friction increases. The dependence of friction on scaling seems to be hinged on the internal structure of granular materials inside the shear band. For engineering applications, peak and residual stresses are both important. We found

that both were dependent on particle size unless the shear box is sufficiently short. The fluctuations of these stresses tend to increase with particle size. The residual stress is more relevant to dense phase processing of granular materials. Thus studying the stability and evolution of structures in shear band will also help to determine the range of frictional values in a given continuously deforming situation.

Other parametric studies were also carried out but not reported here. These studies included the boundary friction effect and the size distribution effect. We investigated a zero friction bottom wall case and found that the degree of particle rotation was strongly influenced by the change of boundary property. We also studied different size distributions from uniform size to a broad standard deviation and found shear band narrowed when the size distribution broadened. These studies show that there is a lot needs to be learnt in order to fully understand the shear band width and particle size effects in a direct shear device.

This study was initiated when HHS and BTH were participating at the NASA/ASEE summer faculty program at the Kennedy Space Center. The first author participated in this project as a visiting research student at Clarkson University.

1 Terzaghi K, Peck R B, Mesri G. Soil Mechanics in Engineering Practice. 3rd ed. New York: Wiley, 1996
2 Leshchinsky D. Design dilemma: Use peak or residual strength of soil. Geotext Geomembranes, 2001, 19: 111－125[doi]
3 Parsons J D. Progress report on an investigation of the shearing resistance of cohesionless soils. In: Proceedings of the 1st International Conference on Soil Mechanics and Foundation Engineering, 1936. 133－138
4 Cerato A B, Lutenegger A J. Specimen size and scale effects of direct shear box tests of sands. Geotech Test J, 2006, 29: 507－516
5 Satake M. Fabric tensors in granular materials. In: Proceedings IUTAM Conference on Deformation and Failure of Granular Materials, Delft, 1982. 63－68
6 Madadi M, Tsoungui O, Lätzel M, et al. On the fabric tensor of polydisperse materials in 2d. Int J Solids Struct, 2004, 41: 2563－2580[doi]
7 Chang C S, Hicher P Y. An elasto-plastic model for granular materials with microstructural consideration. Int J Solids Struct, 2005, 42: 4258－4277[doi]
8 Nicot F, Darve F, RNVO group. A multi-scale approach to granular materials. Mech Mater, 2005, 37: 980－1006
9 Al Hattamleh O, Mühunthan B, Zbib H M. Multi-slip gradient formulation for modeling microstructure effects on shear bands in granular materials. Int J Solids Struct, 2007, 44: 3393－3410[doi]
10 Peters J F, Muthuswamy M, Wibowo J, et al. Characterization of force chains in granular material. Phys Rev E, 2005, 72: 041307[doi]
11 Kuhn M R, Chang C S. Stability, bifurcation, and softening in discrete systems: A conceptual approach for granular materials. Int J Solids Struct, 2006, 43: 6026－6051[doi]
12 Muthuswamy M, Peters J, Tordesillas A. Uncovering the secrets to relieving stress: Discrete element analysis of force chains in particulate media. ANZIAM J, 2006, 47: C355－C372
13 Estrada N, Taboada A. Shear strength and force transmission in granular media with rolling resistance. Phys Rev E, 2008, 78: 021301[doi]
14 Zhang L, Thornton C. DEM simulations of the direct shear test. In: 15th ASCE Engineering Mechanics Conference, Columbia University, New York, 2002
15 Cundall P A, Strack O D L. A discrete numerical model for granular assemblies. Geotechnique, 1979, 29: 47－65[doi]
16 Babic M, Shen H H, Shen H T. The stress tensor in granular shear flows of uniform, deformable disks at high solids concentrations. J Fluid Mech, 1990, 219: 81－118[doi]
17 Mitchell J K. Fundamentals of Soil Behavior. 2nd ed. New York: Wiley, 1993
18 Oda M, Iwashita K. Study on couple stress and shear band development in granular media based on numerical simulation analyses. Int J Eng Sci, 2000, 38: 1713－1740[doi]
19 Mühlhaus H B, Vardoulakis I. The thickness of shear bands in granular materials. Geotechnique, 1987, 37: 271－283[doi]
20 Rechenmacher A L. Grain-scale processes governing shear band initiation and evolution in sands. J Mech Phys Solids, 2006, 54: 22－45[doi]
21 Qin J. Investigation of mechanical properties of geomaterials based on DEM simulation and theories for strain localization analysis. Dissertation for the Doctoral Degree. Dalian: Dalian University of Technology, 2007
22 Iwashita K, Oda M. Rolling resistance at contacts in simulation of shear band development by DEM. J Eng Mech, 1998, 124: 285－292[doi]
23 Bardet J P, Proubet J. The structure of shear bands in idealized granular materials. Appl Mech Rev, 1992, 45: S118－122[doi]
24 Kuhn M R. Structured deformation in granular materials. Mech Mater, 1999, 31: 407－429[doi]
25 Tordesillas A. Force chain buckling, unjamming transitions and shear banding in dense granular assemblies. Philos Mag, 2007, 87: 4987－5016[doi]